Gelsolin Deficiency Blocks Podosome Assembly and Produces Increased Bone Mass and Strength

Meenakshi Chellaiah,* Neil Kizer,* Matthew Silva,‡ Ulises Alvarez,* David Kwiatkowski,‖ and Keith A. Hruska*§

*Renal Division, Department of Medicine, ‡Department of Orthopaedics, and §Department of Cell Biology, Barnes-Jewish Hospital, Washington University, St. Louis, Missouri 63110; and ‖Division of Preventive Medicine, Department of Medicine, Peter Brent Brigham Hospital, Harvard University, Boston, Massachusetts 02115

Abstract. Osteoclasts are unique cells that utilize podosomes instead of focal adhesions for matrix attachment and cytoskeletal remodeling during motility. We have shown that osteopontin (OP) binding to the $\alpha_v\beta_3$ integrin of osteoclast podosomes stimulated cytoskeletal reorganization and bone resorption by activating a heteromultimeric signaling complex that includes gelsolin, $pp^{60c\text{-}src}$, and phosphatidylinositol 3′-kinase. Here we demonstrate that gelsolin deficiency blocks podosome assembly and $\alpha_v\beta_3$-stimulated signaling related to motility in gelsolin-null mice. Gelsolin-deficient osteoclasts were hypomotile due to retarded remodeling of the actin cytoskeleton. They failed to respond to the autocrine factor, OP, with stimulation of motility and bone resorption. Gelsolin deficiency was associated with normal skeletal development and endochondral bone growth. However, gelsolin-null mice had mildly abnormal epiphyseal structure, retained cartilage proteoglycans in metaphyseal trabeculae, and increased trabecular thickness. With age, the gelsolin-deficient mice expressed increased trabecular and cortical bone thickness producing mechanically stronger bones. These observations demonstrate the critical role of gelsolin in podosome assembly, rapid cell movements, and signal transduction through the $\alpha_v\beta_3$ integrin.

Key words: gelsolin • phosphatidylinositol 3′-kinase • actin • podosomes • osteoclasts

Introduction

Osteoclasts are characterized by unique cell adhesion structures found in highly motile cells called podosomes, a property they share with several types of cancer cells and monocyte and/or macrophages. When osteoclasts are cultured on glass surfaces, multiple rows of podosomes are localized in the area corresponding to the clear zone in osteoclasts (Marchisio et al., 1984; Turksen et al., 1988; Zambonin-Zallone et al., 1989; Lakkakorpi and Vaananen, 1991; Teti et al., 1991). Signaling molecules associated with podosomes such as $pp^{60c\text{-}src}$ (Boyce et al., 1992; Schwartzberg et al., 1997), phosphatidylinositol 3′-kinase (PI3-K)[1] (Buck and Horwitz, 1987; Lakkakorpi et al., 1997; Nakamura et al., 1997), and rhoA (Zhang et al., 1995; Maejima-Ikeda et al., 1997) have been shown to be essential for cytoskeletal organization and bone resorption. Osteoclasts from $src^{-/-}$ mice have an altered actin distribution with no peripheral podosome arrangement (Schwartzberg et al., 1997), which is similar to $pp^{60c\text{-}src}$ antisense oligonucleotide treatment of cells (Chellaiah et al., 1998). Podosomes consist of an F-actin core surrounded by the actin-binding proteins vinculin, talin, and α-actinin (Marchisio et al., 1984). The presence of gelsolin in osteoclast podosomes is known but its function is not (Zambonin-Zallone et al., 1983, 1989; Marchisio et al., 1984, 1987; Lakkakorpi and Vaananen, 1991).

Gelsolin, an actin-binding protein, controls the length of actin filaments in vitro, and cell shape and motility in vivo by a variety of mechanisms (Cunningham et al., 1991). Gelsolin severs assembled actin filaments, caps the fast-growing plus ends, and promotes growth of actin filament by creating nucleation sites (Stossel, 1989). Severing and capping are regulated by calcium ions and pH, which synergistically activate gelsolin's binding to actin. Binding of gelsolin to phosphoinositides causes the release of gelsolin from the filament end (uncapping), providing a site for rapid monomer addition (Janmey and Stossel, 1987; Janmey et al., 1987).

Address correspondence to Keith A. Hruska, Renal Division, Barnes Jewish Hospital North, Washington University, 216 South Kingshighway, St. Louis, MO 63110. Tel.: (314) 454-7771. Fax: (314) 454-5126. E-mail: khruska@imgate.wustl.edu

[1]*Abbreviations used in this paper:* $Gsn^{-/-}$, $Gsn^{+/+}$, gelsolin-null and wild-type mice, respectively; OP, osteopontin; PI3-K, phosphatidylinositol 3′-kinase; TRAP, tartrate-resistant acid phosphatase.

In avian osteoclasts, we have shown previously that osteopontin (OP) binding to integrin $\alpha_v\beta_3$ in osteoclasts stimulates gelsolin-associated PI3-K, leading to increased levels of gelsolin-associated polyphosphoinositides such as phosphatidylinositol 4,5-bisphosphate, phosphatidylinositol 3,4-bisphosphate, phosphatidylinositol 3,4,5,-trisphosphate, uncapping of actin barbed ends, and actin filament formation. Inhibition of PI3-K blocks OP-stimulated actin filament formation, and cell motility (Chellaiah and Hruska, 1996). Recently, we have demonstrated that OP stimulation of gelsolin-associated $pp^{60c\text{-}src}$ is upstream of PI3-K. Antisense oligonucleotides to $pp^{60c\text{-}src}$ blocked OP stimulation of gelsolin-associated PI3-K as well as the downstream effects on the cytoskeleton and bone resorption (Chellaiah et al., 1998).

Gelsolin-deficient ($Gsn^{-/-}$) mice, generated by gene targeting methods (Witke et al., 1995), express mild physiological dysfunction during hemostasis, inflammation, and possibly skin remodeling, but gelsolin was not required for oocyte development, spermatogenesis, embryonal development, or longevity. $Gsn^{-/-}$ dermal fibroblasts have excessive actin stress fibers and migrate more slowly than wild-type ($Gsn^{+/+}$) fibroblasts, but have increased contractility in vitro (Witke et al., 1995). The skeleton of $Gsn^{-/-}$ mice has not been formally analyzed, but tooth eruption and bone development appear normal. Bone cells from $Gsn^{-/-}$ mice have not been studied.

We show here that elimination of gelsolin resulted in osteoclasts devoid of podosomes and actin rings. Mechanisms of cell attachment substituting for podosomes were expressed, but these failed to support cell motility. However, they were sufficient to enable cell polarization and bone resorption. $Gsn^{-/-}$ osteoclasts failed to respond to OP with stimulation of motility and bone resorption. Endochondral bone formation was abnormal with delayed resorption of calcified cartilage and thicker metaphyseal trabeculae. Adult $Gsn^{-/-}$ mice developed thicker cortical and trabecular bone, which was more resistant to fracture, compatible with a mild imbalance between bone resorption and formation.

Materials and Methods

Rhodamine phalloidin was obtained from Molecular Probes. All the other chemicals, including antigelsolin antibody, were purchased from Sigma Chemical Co.

Coculture and Generation of Murine Osteoclasts In Vitro

Mouse osteoclasts were generated in vitro using the mouse bone marrow and stromal cell coculture system essentially as described (Shioi et al., 1994). After coculture for 6–9 d, ST2 cells were removed by treatment with collagenase and dispase (1 mg/ml each in PBS) at 37°C for 20 min as described (Wesolowski et al., 1995). After washing the cultures with PBS, all of the ST2 cells (99%) were removed. The remaining attached cells were rinsed with PBS, and the cultures were kept in cell dissociation buffer for an additional 5 min. Cells were removed from the plates by gentle scraping. Some of the removed cells were replated and stained with either trypan blue or for tartrate-resistant acid phosphatase (TRAP). Cells excluded trypan blue, and they were 99% TRAP-positive. These TRAP-positive cells were used for migration and bone resorption assays as described below.

Actin Staining

The mouse osteoclasts generated in cocultures were placed in 6-well clusters containing glass coverslips. Osteoclasts attached to the plates and were treated with OP (25 μg/ml) or vehicle as described previously (Chellaiah and Hruska, 1996). Actin staining was carried out as described previously (Chellaiah et al., 1998).

Measurement of F-Actin Content Using Rhodamine-Phalloidin Binding

Osteoclasts were made as described above. After coculture for 6–9 d, ST2 cells were removed by treatment with collagenase and dispase (1 mg/ml each in PBS) at 37°C for 20 min as described (Wesolowski et al., 1995). Plates were washed two to three times with serum-free α-MEM medium and the remaining attached cells were kept in serum-free α-MEM medium for 2 h. Cells were treated with PBS or OP for 15 min. For each treatment four to six wells were used. The cells were fixed and rhodamine-phalloidin binding to F-actin was done as described (Chellaiah and Hruska, 1996; Chellaiah et al., 1998).

Cell Migration Assays

Phagokinesis. Substrates such as recombinant chicken OP, vitronectin, or fibronectin were diluted in PBS and used for phagokinesis assays, which were performed in 6-well tissue culture dishes. Colloidal gold particles were made essentially as described (Takahashi et al., 1995). Osteoclasts isolated (see above) were seeded at low density (10^3 cells/well). Once the cells were attached to the wells, the substrates were added as soluble protein (OP, 25 μg/ml; vitronectin or fibronectin, 10 μg/ml) in α-MEM containing 1% serum and 2% BSA. Some wells were treated with an antibody to OP (50 μg/ml) and OP (25 μg/ml). The cells migrated on this substrate, and phagocytized the gold particle to produce a white track free of the particle in a time-dependent manner. The migrating cells were visible as a black body (Takahashi et al., 1995). Areas were measured after 14-h incubations with the proteins. Cell motility was evaluated by measuring the areas free of gold particles. By using a grided reticule (Boyce Scientific, Inc.) in the eyepiece of a Nikon microscope, areas free of gold particles were measured using a 10× objective. Areas free of gold particles were represented as area moved in mm^2.

Haptotaxis (Transwell Migration) Assay. To assay cell migration, Transwell migration chambers (8-μm pore size) were used (Senger et al., 1996). Undersides of the membranes were coated with vitrogen 100 (collagen type 1; 30 mg/ml) at room temperature for 2 h according to the manufacturer's instructions. Osteoclasts isolated as described above were pelleted and resuspended in α-MEM medium containing 1% serum and 2% BSA (50,000 cells/ml). Cells were added to the upper chamber in the above mentioned medium (100 μl) and substrates like OP (25 μg/ml) or vitronectin or fibronectin (10 μg/ml) were added to the lower chamber in α-MEM medium containing 1% serum and 2% BSA (600 μl). Cell migration was allowed to proceed at 37°C in a standard tissue culture incubator for 12–14 h. Cells that migrated to the undersides were stained, visualized, and counted as described (Senger et al., 1996). Data are presented as the number of migrated cells field (mean ± SEM) and all assays were performed in quadruplicate. Statistical significance was calculated as mentioned below in data analysis.

Bone Resorption Assay

Whale dentine slices (1.5 cm^2 in size and 0.75 mm in thickness) were cut from previously prepared rectangular sticks on a low-speed saw and were stored in 70% ethanol until required. Before being used in a resorption assay, the slices were sonicated for 3–5 min in distilled water and washed for 2 h in two changes of fresh distilled water. The slices were resterilized in fresh 70% ethanol and placed into wells of a 48-well tissue culture plate. After three washes with α-MEM serum-free media, the slices were placed overnight in a 37°C incubator in the same media. The osteoclast suspension (2×10^4 cells) was added to each well, and after 2 h of adherence the culture media were replaced with α-MEM containing either vehicle (PBS) or 25 μg/ml mouse OP expressed in bacteria. After incubation for 48 h, cells were scraped from the slices and the slices were washed 7–10 times with water. Pits were stained with acid hematoxylin (Sigma Chemical Co.) for 6 min, washed well with water, and counted. The number of pits was determined microscopically. The effect of test substances on bone resorption was determined by scanning the pit areas and pit depth as described below.

Measurement of Pit Area and Depth

Photomicrographs were obtained with the Zeiss LSM 410 scanning laser

confocal microscope system, which employs a Zeiss 135 Axiovert inverted microscope fitted with an Omnicron Argon/Krypton laser for confocal excitation. The dentine slices mounted on No. 1 coverslips were viewed with a 40 × 0.6 NA air objective. Images were recorded in the epi-reflection mode using the 488-nm line of the argon laser in a 512 × 512 pixel format. Data collection and processing were accomplished with the Zeiss LSM 410 software package. Photomicrographs were produced from a Sony Mariograph color video printer or stored in a TIFF image format for post collection image processing. An XY digital image of each pit was first obtained. The area of the pit was determined from the free-hand traced perimeter using the LSM software Area Measurement function. The depth profile of the pit was obtained using the LSM Z Scan function to form an XZ profile. The maximum pit depth was determined from this scan using the LSM software Distance Measurement function. All depth measurements were corrected for the presence or absence of immersion oil.

Immunostaining

Osteoclasts cultured on whale dentine slices or glass coverslips were immunostained with an antibody (E11; kindly provided by Dr. Stephen Gluck, University of Florida College of Medicine, Gainesville, FL) to 31-kD subunit of vacuolar H+ ATPase (Hemken et al., 1992) or gelsolin antibody as described (Wu et al., 1991; Chellaiah et al., 1996). In brief, cells were fixed with 3% paraformaldehyde and permeabilized with 10 mM Tris-HCl, pH 7.4, 150 mM NaCl, and 1 mM $CaCl_2$ containing 0.1% Triton X-100 for 1 min. The cells were washed and incubated with E11 antibody or gelsolin antibody (1:100 dilution) for 2 h, washed, and counter stained with Cy2-conjugated goat anti–mouse IgG for 2 h. The cells were washed and mounted on a slide in a mounting solution (Vector Laboratories, Inc.). The cells were viewed on a Zeiss LSM 410 confocal laser scanning microscope and photomicrographs were obtained as described (Gupta et al., 1996). Images were recorded as described below.

Lysate Preparation and Western Analysis

After ST2 cells were removed as described above in osteoclast preparation, cells were washed three times with ice-cold PBS and lysates were made from osteoclasts derived from $Gsn^{-/-}$ and $Gsn^{+/+}$ mice as described previously (Chellaiah and Hruska, 1996). Protein contents were measured using the Bio-Rad protein assay reagent kit. Equal amounts of lysate proteins were immunoprecipitated with an antibody to gelsolin (Sigma Chemical Co.) or nonimmune serum. Immunoprecipitations and Western analysis were carried out as described (Chellaiah and Hruska, 1996).

Immune Complex Kinase Assay Analysis for src and PI3-K

Equal amounts of protein lysates made from PBS or OP-treated cells were immunoprecipitated with an antibody to gelsolin. The immunecomplexes, adsorbed to protein A–Sepharose pellets, were assayed for $pp^{60\text{-}src}$ or lipid kinase (PI3-K) activity as described previously (Chellaiah and Hruska, 1996; Chellaiah et al., 1998).

Polarization of the H+ ATPase in $Gsn^{-/-}$ Osteoclasts

Images were collected on the Zeiss laser scanning confocal system in the dual imaging mode. One detector was set to image in FITC fluorescence (488 nm laser line excitation, 515–540 nm FITC emission), and the second detector was set to record the backscattered epi-reflection image using the 568-nm laser line. The two images were collected simultaneously. The green FITC fluorescence image was stored in the green frame, and the 568-nm epi-reflection image was stored in the red frame. The composite color image was viewed as green fluorescence plus red epi-reflection.

Bone Histomorphometry

The distal tibia were fixed in phosphate-buffered 10% formalin, pH 7.4, and decalcified in 14% EDTA for 10–14 d. The bones were washed sequentially with 50, 70, and 90% ethanol and embedded. 5-μm thick longitudinal sections were made and stained with toluidine blue stain or TRAP staining to identify osteoclasts. To estimate mineral opposition rate and bone formation rate, mice were injected with calcein at 2 and 5 d before sacrificing. The distal right femur was kept in 90% ethanol and embedded. Longitudinal sections were made. Static and dynamic histomorphometric measurements were made using a computer and digitizer tablet (Osteomeasure; Osteometrics Inc.) interfaced to a Leitz microscope (Leitz Wetzlar) with a drawing tablet. All measurements were done to the metaphyseal region distal to the growth plate region. To estimate bone formation rate, double labeled and single labeled areas were traced and calculated as described (Jilka et al., 1996; Weinstein et al., 1997). Terminology used is that recommended by the Histomorphometry Nomenclature Committee of the American Society of Bone and Mineral Research (Parfitt et al., 1987).

Mechanical Properties of the Femora from $Gsn^{+/+}$ and $Gsn^{-/-}$ Mice

The left femora from 16 mice was designated for biomechanical testing. Femora were isolated, cleaned of soft tissues, wrapped in gauze that was soaked with PBS, wrapped again in plastic, placed in a sealed vial, and stored at –20°C until testing. Before testing, specimens were thawed to 23°C. Four-point bending tests were conducted using a materials testing machine (8500R; Instron) fitted with an appropriate load transducer (111 N force cell; Lebow 3397). Tests were conducted using a four-point fixture with a 9-mm spacing between the outer (support) points and a 4-mm spacing between the inner (loading) points. The bones were flexed in the anterior-posterior plane (Jepsen et al., 1996). The inner points were displaced at a constant rate of 0.03 mm/s. Torque rotation and force displacement data were collected using a computerized data acquisition system (Labview 5.0; National Instruments).

After testing, force values (F) from the bending tests were converted to bending moment values (M) using the relation M = Fa/2, where a was the distance between the outer and inner points (2.5 mm). Displacement data were normalized by a geometric factor to allow direct comparison between other experiments done using different testing geometries. Displacement values were divided by (3aL − 4a2)/6, where L is the distance between the outer points. From the moment versus normalized displacement curves, four parameters were computed: ultimate moment (Nmm), bending rigidity (Nmm^2), displacement at failure (mm/mm^2), and energy to failure ($Nmm \times [mm/mm^2]$). Failure was defined at the point of ultimate (maximum) moment, whereas bending rigidity was defined as the slope of the linear region of the curve.

Data Analysis

All comparisons were made as "% control", which refers to vehicle-treated cells. The other treatment groups in each experiment were normalized to each control value. Data presented are mean ± SEM of experiments done at different times normalized to intraexperimental control values. For statistical comparisons, analysis of variance (ANOVA) was used with the Bonferroni corrections (Instat for IBM, version 2.0; Graphpad software).

Results

Analysis of the Actin Cytoskeleton of $Gsn^{+/+}$ and $Gsn^{-/-}$

As shown in Fig. 1 (upper panels) and Fig. 2 (+/+ PBS), osteoclasts plated on glass coverslips arranged their actin cytoskeleton in peripheral rows of dot-like structures (podosomes). In some cells, podosomes were further organized into actin ring–like structures found in actively resorbing osteoclasts (Fig. 2, PBS +/+) (Taylor et al., 1989; Kanehisa et al., 1990; Lakkakorpi et al., 1993; for review see Horton et al., 1996). Podosomes were not observed in $Gsn^{-/-}$ osteoclasts (Fig. 1, lower panels). Instead, F-actin was present in a peripheral web-like structure, which was often bipartite (Fig. 2, lower panels) or present diffusely throughout the cell as seen in the higher magnification (Fig. 1, lower panels). The peripheral row of dot-like structures was never observed in $Gsn^{-/-}$ osteoclasts.

Effect of OP on Actin Cytoskeleton Organization

When osteoclasts from $Gsn^{+/+}$ mice were treated with OP,

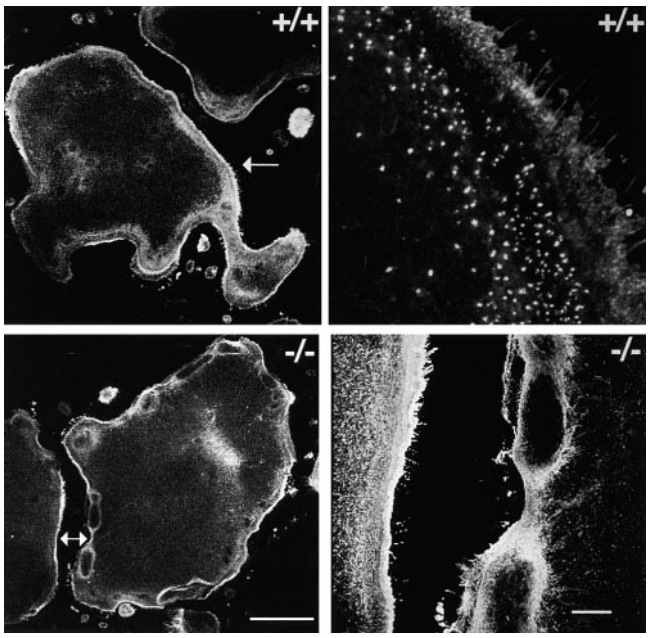

Figure 1. High-power examination of the actin cytoskeleton of $Gsn^{+/+}$ and $Gsn^{-/-}$ osteoclasts. Osteoclasts cultured on glass coverslips were fixed and stained with rhodamine-phalloidin. Cells were examined by confocal microscopy. The actin cytoskeleton of $Gsn^{-/-}$ osteoclasts (lower panels) was distinctly altered compared with the $Gsn^{+/+}$ cells (upper panels). The arrows indicate areas of the cytoskeleton shown at higher magnification (right, upper and lower panels). Bars, 100 μm (left panels); 10 μm (right panels).

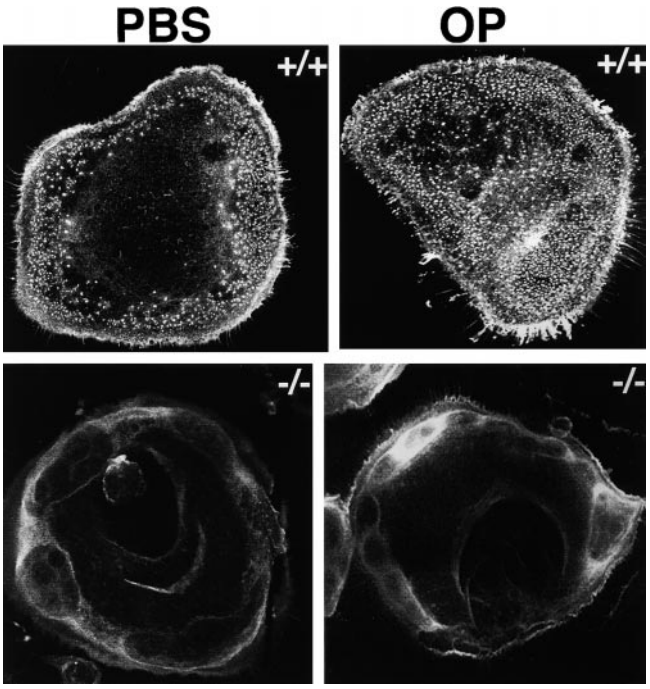

Figure 2. The effect of OP on the actin cytoskeleton. Osteoclasts were fixed and stained with rhodamine-phalloidin. Actin filament organization in cells treated with PBS or OP is shown. Cells were examined by confocal microscopy. The actin staining of osteoclasts derived from wild-type (+/+) and null (−/−) mice are shown.

the entire cell subsurface was occupied with podosomes within 15 min (Fig. 2, OP +/+). Conversely, OP treatment had no effect on the cytoskeleton of the $Gsn^{-/-}$ osteoclasts (Fig. 2, OP −/−). In contrast to the podosomes of osteoclasts derived from $Gsn^{+/+}$ mice, the actin cytoskeleton of $Gsn^{-/-}$ osteoclasts demonstrated either an actin web (Fig. 2, lower panels) or a diffuse distribution throughout the cell (Fig. 1). Discrete dot-like podosome structures were never observed in either type of $Gsn^{-/-}$ osteoclasts.

Analysis of Expression of Gelsolin in Osteoclasts

Gelsolin is an actin capping protein of podosomes (Zambonin-Zallone et al., 1983, 1989; Marchisio et al., 1984, 1987). Immunostaining of osteoclasts derived from cells of wild-type mice with antigelsolin antibody showed that gelsolin was strongly colocalized with actin in podosomes (Fig. 3 A, $Gsn^{+/+}$) and colocalized along the inner edge of actin ring–like structures (Fig. 3 A, $Gsn^{+/+}$). Immunostaining of osteoclasts isolated from $Gsn^{-/-}$ mice documented the absence of gelsolin expression in the $Gsn^{-/-}$ mice (Fig. 3 A, $Gsn^{-/-}$). The few green spots observed in the $Gsn^{-/-}$ mice are either nonspecific or bleed through from the red channel. In addition, Western analysis of the antigelsolin immunoprecipitates made from the lysates of $Gsn^{-/-}$ osteoclasts demonstrates the absence of gelsolin (Fig. 3 B, lane 2).

Measurements of F-Actin Levels

F-actin levels were measured in both $Gsn^{+/+}$ and $Gsn^{-/-}$ mice to detect any increase in F-actin content due to the severing activity by any other protein. Since it has been shown that Cap 32/34 and CapG are expressed in appreciable levels in embryonic cells, and that these proteins may function in capping and uncapping of actin filaments, we wanted to see whether these proteins can increase the F-actin content of the cells. Platelets isolated from $Gsn^{-/-}$ mice demonstrated diminished capping and severing activities. The resting level actin filaments were similar in osteoclasts derived from $Gsn^{+/+}$ and $Gsn^{-/-}$ mice (Fig. 4). OP treatment produced a threefold increase in F-actin in $Gsn^{+/+}$ osteoclasts and produced no change in $Gsn^{-/-}$ osteoclasts (Fig. 4). The increases in F-actin seen in murine osteoclasts in response to OP is similar to those observed in avian osteoclasts (Chellaiah and Hruska, 1996), except that the F-actin change was distributed as podosomes in the mouse and as stress fibers in the avian osteoclasts. Consistent with our previous observation, vinculin, α-actinin, profilin, or CapG had no effect on actin filament formation (Chellaiah and Hruska, 1996).

Analysis of Signaling Molecules Associated with Gelsolin, and the Effects of OP

We have shown previously that binding of OP to $\alpha_v\beta_3$ stimulated association signal generating molecules with gelsolin in avian osteoclasts (Chellaiah and Hruska, 1996; Chellaiah et al., 1998). To see whether OP stimulation in mouse osteoclasts produced similar activation as seen in avian osteoclasts, in vitro kinase assays were performed on the immune complexes generated by using a gelsolin anti-

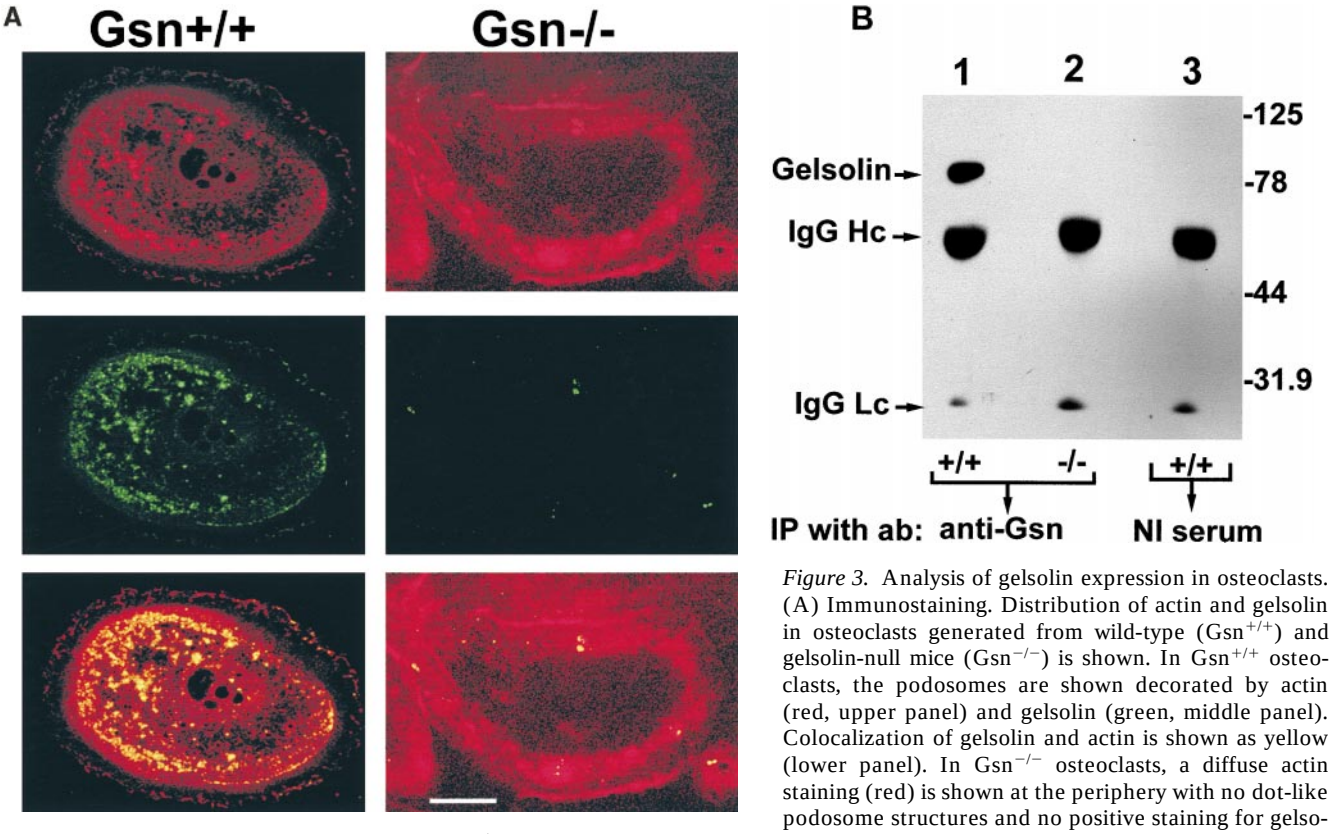

Figure 3. Analysis of gelsolin expression in osteoclasts. (A) Immunostaining. Distribution of actin and gelsolin in osteoclasts generated from wild-type ($Gsn^{+/+}$) and gelsolin-null mice ($Gsn^{-/-}$) is shown. In $Gsn^{+/+}$ osteoclasts, the podosomes are shown decorated by actin (red, upper panel) and gelsolin (green, middle panel). Colocalization of gelsolin and actin is shown as yellow (lower panel). In $Gsn^{-/-}$ osteoclasts, a diffuse actin staining (red) is shown at the periphery with no dot-like podosome structures and no positive staining for gelsolin (green, middle panel). Few spots seen in $Gsn^{-/-}$ osteoclasts are either nonspecific or due to bleed through from the red channel. Bar, 25 μm. (B) Western analysis. Gelsolin is present in the immunoprecipitate from wild-type (+/+, lane 1) mice and not in null (−/−, lane 2) mice or in the nonimmune serum immunoprecipitate (lane 3) from +/+ osteoclast.

body. In vitro immune complex kinase assays for $pp^{60c\text{-}src}$ have demonstrated that OP induced an increase in phosphorylation of $pp^{60c\text{-}src}$ (Fig. 5, A and B) and increased its activity towards phosphorylating an exogenous substrate, casein (Fig. 5 B). In addition, phosphorylation of two other proteins with the molecular masses of 125 kD (Fig. 5, A and B) and 85 kD (Fig. 5 B) was observed. p85 protein was identified as PI3-K in avian osteoclasts (Chellaiah and Hruska, 1996). Coimmunoprecipitation of PI3-K with gelsolin was further confirmed by a PI3-K assay (Fig. 5 C). OP stimulation of PI3-K activity associated with gelsolin is evident from the phosphorylation of the exogenous substrate, phosphatidylinositol 4,5-bisphosphate to phosphatidylinositol 3,4,5-trisphosphate (Fig. 5 C).

Analysis of Vinculin Distribution

Immunolocalization of vinculin was performed in $Gsn^{+/+}$ and $Gsn^{-/-}$ osteoclasts to further define their adhesion structures. Vinculin is involved in assembling focal adhesion plaques and mediating anchorage to the cytoskeleton (Steimle et al., 1999). It has also been shown to have regulatory roles in adhesion, spreading, and motility of cells in culture (Xu et al., 1998; Rodriguez Fernandez et al., 1992, 1993). In the $Gsn^{+/+}$ osteoclasts (Fig. 6, PBS +/+), vinculin was arrayed peripherally, forming a double band with areas of actin ring structure between the double band. These results are in agreement with prior studies in rat and avian osteoclasts (Taylor et al., 1989; Lakkakorpi et al., 1993). In areas of peripheral podosomes, vinculin was organized in a single intense band at the cell periphery and in the podosome structures. After OP treatment, changes in vinculin distribution (Fig. 6, OP +/+) lagged behind those of actin (Fig. 1), gelsolin (Fig. 3), and the $\alpha_v\beta_3$ inte-

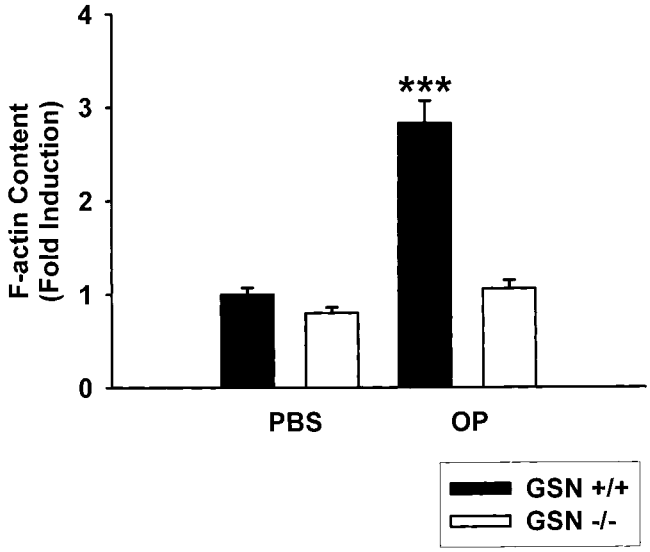

Figure 4. The effect of OP treatment on F-actin content of $Gsn^{+/+}$ and $Gsn^{-/-}$ osteoclasts. F-actin content of wild-type ($Gsn^{+/+}$, PBS) osteoclasts was increased threefold by treatment with OP ($Gsn^{+/+}$, OP). No effect of OP on F-actin levels was seen in the gelsolin-eficient ($Gsn^{-/-}$, PBS and $Gsn^{-/-}$, OP) osteoclasts. Asterisks indicate that data are mean ± SEM ($n = 3$), $P < 0.001$.

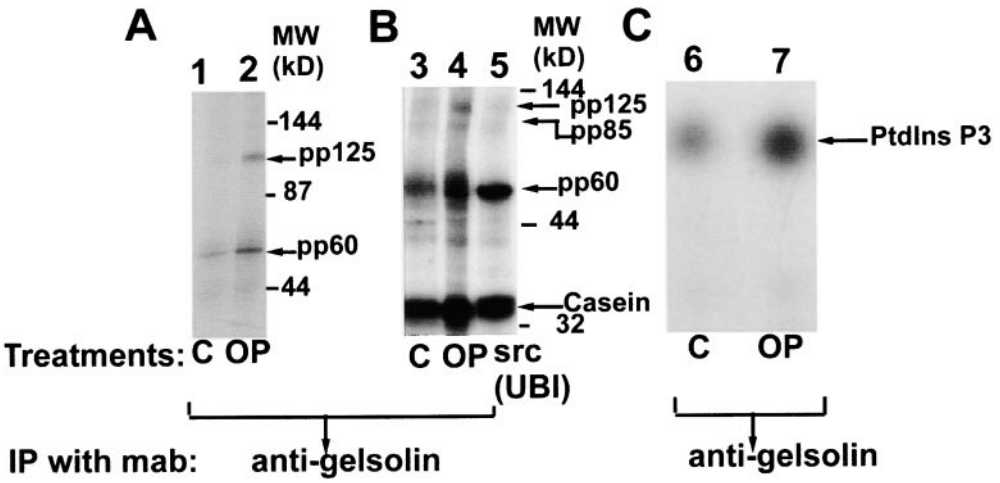

Figure 5. The effect of OP on phosphorylation of proteins associated with gelsolin. (A) In vitro protein kinase assay without casein as exogenous substrate and (B) with casein as exogenous substrate. Phosphorylation of protein with molecular masses of 125, 85, and 60 kD is shown by arrows in A and B. Phosphorylation of casein is shown in B. Phosphorylation of casein is increased by OP treatment. (C) Effect of OP on gelsolin-associated PI3-K activity. Autoradiogram of the TLC plate is shown. OP-stimulated phosphatidylinositide 3,4,5-trisphosphate (PtdIns P3) formation is shown by arrow. Treatments are shown below the figure.

grin (data not shown), which were dramatically redistributed at 15 min. Vinculin was detected in the newly formed podosomes of the OP-treated $Gsn^{+/+}$ osteoclasts, probably translocating from an intracellular pool different from the formed adhesion structures. In $Gsn^{-/-}$ osteoclasts, vinculin was also arrayed peripherally in discrete attachment sites with a unique structure not resembling podosomes or focal adhesions (Fig. 6, middle panels). In $Gsn^{-/-}$ osteoclasts with a diffuse actin distribution as in Fig. 1, vinculin was also arrayed diffusely with discrete attachment sites scattered throughout the cells (Fig. 6, lower panels).

Analysis of Osteoclast Motility

Since retraction of filopodia is delayed in the growth cones of $Gsn^{-/-}$ neurons (Lu et al., 1997), and $Gsn^{-/-}$ leukocytes and fibroblasts are hypomotile in vitro (Witke et al., 1995), we examined the motility of osteoclasts derived from $Gsn^{-/-}$ bone marrow cells. In phagokinesis assays, the distance migrated by $Gsn^{+/+}$ osteoclasts was stimulated threefold by exogenous addition of OP (Fig. 7 A). Whereas basal phagokinesis of $Gsn^{-/-}$ osteoclasts did not differ from wild-type, OP addition failed to stimulate migration (Fig. 7 A). In haptotaxis assays, the basal motility represents the ability of the cell to sense and respond to an adhesion substrate as opposed to the random movements in the phagokinesis assays. The motility of $Gsn^{-/-}$ osteoclasts was severely impaired, and again, there was a lack of response to the chemotactic factor, OP (Fig. 7 B). The rate of motility is related to the amount of F-actin levels in the cells. It has been shown that migrant fibroblast cells showed increased actin levels in response to serum levels (Arora and McCulloch, 1996). We have shown previously in avian osteoclasts increased F-actin levels in response to OP (Chellaiah and Hruska, 1996; Chellaiah et al., 1998). In this study, we have shown that OP increased the F-actin levels and migration of osteoclasts isolated from $Gsn^{+/+}$ mice, whereas OP had no effect on osteoclasts from $Gsn^{-/-}$ mice.

In Vitro Bone Resorption Assay

Bone resorption appears to proceed by the intricate coordination of several processes, including attachment, polarized secretion of acid and proteases, and active motility of osteoclasts along the bone surface (Kanehisa and Heersche, 1988; Blair et al., 1989; Zambonin-Zallone et al., 1989). Even though osteoclasts isolated from $Gsn^{-/-}$ mice attach and spread well on glass coverslips and bone, the polarization efficiency was measured by immunostaining the osteoclasts with an antibody to the H^+ ATPase proton pump responsible for mineral dissolution (Hemken et al., 1992). Osteoclasts derived from $Gsn^{-/-}$ cells were cultured on dentine slices, and the H^+ ATPase, which is found in the ruffled border overlying resorption pits, was found to be concentrated at this location (Fig. 8). This indicates that signals for the osteoclasts to polarize are normal. Secondly, we analyzed the number and size of resorption pits produced in the basal conditions (PBS). The number of resorption pits was similar between $Gsn^{+/+}$ and $Gsn^{-/-}$ mouse osteoclasts (Fig. 9 A). Compilation of pit area (XY) and pit depth (XZ) using confocal microscopy scans (Fig. 9 B) on multiple dentine slices with osteoclasts from multiple preparations (Table I) revealed competency of the $Gsn^{-/-}$ cells in basal conditions. However, response of $Gsn^{-/-}$ osteoclasts to OP treatment was absent, whereas pit complexity, pit area, and pit depth

Table I. Quantitation of Bone Resorption by Mouse Osteoclasts In Vitro

	$Gsn^{+/+}$		$Gsn^{-/-}$	
Parameter	PBS	OP	PBS	OP
Pit depth (μm)	13 ± 0.8	36 ± 8*	14 ± 4.3	15 ± 2.6
Pit area (μm^2)	1,386 ± 233	5,201 ± 952*	1,265 ± 265	1,671 ± 218

About 20–25 pits/slice and four slices from each experiment were scanned (as shown in Fig. 8 B). Data shown are mean ± SEM of three experiments.
*$P < 0.001$ for pit depth and pit area.

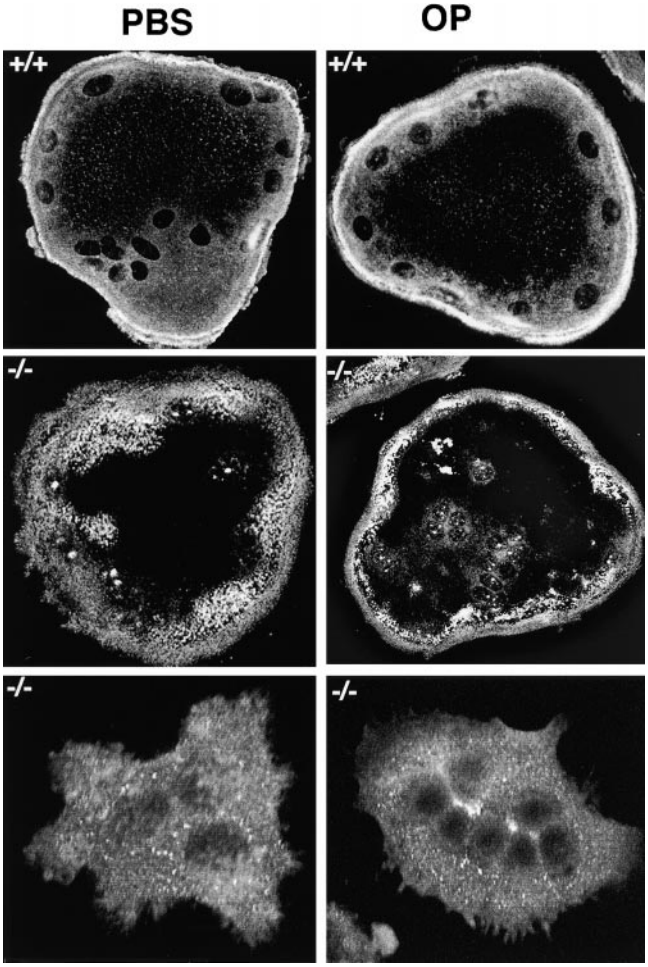

Figure 6. Vinculin distribution in $Gsn^{+/+}$ and $Gsn^{-/-}$ osteoclasts. In $Gsn^{+/+}$ osteoclasts, vinculin was arrayed in often dual rows bordering actin rings shown here as the unstained ring between the vinculin (+/+). Two types of vinculin distribution were observed in the $Gsn^{-/-}$ osteoclasts: a peripheral distribution intermixed in the actin mesh (middle panels, +/+), or a diffuse distribution (lower panels, −/−).

were increased in $Gsn^{+/+}$ osteoclasts (Fig. 9 A and Table I). Since OP is a chemotactic factor, bone resorption in vivo probably proceeds under the influence of this factor regulating the direction of osteoclast motility. Thus, the lack of response to OP may reflect a diminished capacity for bone resorption in vivo.

Skeletal Phenotype of the $Gsn^{-/-}$ Mice

Under laboratory conditions, the homozygous mutant mice remained healthy for at least 18 mo and showed normal somatic development and reproductive capacity. They behaved as expected and appeared to hear normally upon startling. Skeletal radiographs revealed no deformity of the long bones and are not shown. There was a detectable increase in cortical thickness of the tibial and femoral diaphysis at age 14 wk (Table II), but this was not apparent at 3 or 9 wk of age. Despite this increase in diaphyseal thickness, femoral lengths were not different, and the club-like deformities reported in other osteopetrotic mutations (Marks, 1989; Hayman et al., 1996) were absent.

Table II. Histomorphometry of Bones from Wild-type and $Gsn^{-/-}$ Mice

	$Gsn^{+/+}$	$Gsn^{-/-}$
Tibial histomorphometry		
Cancellous bone area (%)	24.8 ± 3.37	42.2 ± 3.18§
Trabecular spacing (μm)	139 ± 16.3	105 ± 23.7
Trabecular number (number/mm)	5.61 ± 0.47	6.10 ± 0.86
Trabecular thickness (μm)	45.8 ± 6.96	76.9 ± 8.13‡
Osteoblast perimeter (number/Bpm)	1.94 ± 0.35	2.40 ± 0.40
Number of osteoblasts	296 ± 68	284 ± 58
Number of osteoclasts	149 ± 4	223 ± 32
Eroded perimeter (number/Bpm)	1.78 ± 0.40	0.74 ± 0.18*
Osteoclast perimeter (number/Bpm)	1.83 ± 0.35	2.90 ± 0.37
Mineral appositional rate ($\mu m^2/\mu m/d$)	0.51 ± 0.1	1.1 ± 0.3*
Bone formation rate/Bpm ($\mu m^2/\mu m/d$)	0.22 ± 0.04	0.36 ± 0.13
Femoral histomorphometry		
Cortical width (μm)	202 ± 9.72	238 ± 12.6*

Data shown are mean ± SEM. There are four to six animals per group.
*$P < 0.05$.
‡$P < 0.01$.
§$P < 0.005$.

To assess skeletal histomorphometry, mice were injected with calcein to label areas of bone mineralization on two occasions, and histomorphometry of nondecalcified and decalcified bone sections was performed as described in Materials and Methods. Bone sections were stained for cartilage proteoglycans with toluidine blue, and for TRAP to aid in detection of osteoclasts. As shown in Fig. 10, at 14 wk of age the chondrocytes of the epiphyseal growth plates were reduced in number, mildly disorganized, and the cartilage matrix was expanded. The bone trabeculae in the metaphyses below the primary spongiosa of $Gsn^{-/-}$ mice had retained cartilage proteoglycan detected by the toluidine blue stain. Furthermore, the metaphyseal trabeculae of $Gsn^{-/-}$ bones (Fig. 10, A and C, arrowheads) were thicker as confirmed by formal histomorphometric measurements (Table II). Osteoclast numbers and osteoclast perimeters in the metaphyses tended to be higher in the bones from $Gsn^{-/-}$ mice, as shown in the sections stained for TRAP (Fig. 10 B). This increase was not statistically significant (Table II), but it may have been adaptive for the decreased bone resorption. The intensity of the TRAP stain did not differ between wild-type and mutant osteoclasts. The decrease in bone resorption of mutant mice was demonstrated by changes in eroded perimeters. The perimeters of eroded surfaces were significantly reduced in $Gsn^{-/-}$ mice ($P < 0.05$), demonstrating that osteoclast-mediated bone resorption was diminished.

The cancellous bone area ($P < 0.005$) and trabecular thickness ($P < 0.01$) were significantly higher in $Gsn^{-/-}$ bones as compared with those from $Gsn^{+/+}$ mice (Table II). The impact of gelsolin deficiency was not limited to trabecular bone, as cortical bone assessed in the middiaphyseal femoral midshaft was increased in width ($P < 0.05$) (Table II). The increase in bone mass was age-dependent and not detected until after 9 wk. Age-related skeletal abnormalities of bone thickness and mineralization have been noted previously in mild osteopetrosis (Hayman et al., 1996). The increase in bone mass reported here probably resulted from the defect in bone resorption and the normal rates of bone formation producing an imbalance in skeletal remodeling similar to that reported in

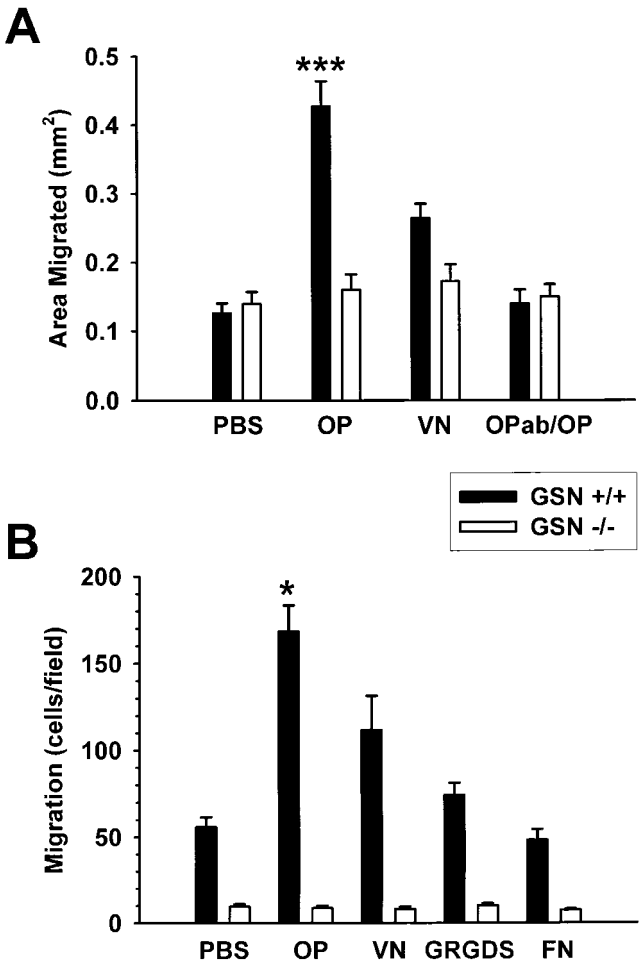

Figure 7. Effect of OP on the motility of $Gsn^{+/+}$ and $Gsn^{-/-}$ osteoclasts. Osteoclast motility was assessed in vitro during both phagokinesis (A) and haptotaxis (B) assays. OP increased motility of $Gsn^{+/+}$ osteoclasts more than twofold in both assays, and had no effect on the motility of $Gsn^{-/-}$ osteoclasts. Likewise vitronectin (VN) stimulated osteoclast motility, whereas GRGDS and fibronectin (FN) had no effect. None of these proteins stimulated $Gsn^{-/-}$ osteoclast motility. Furthermore, in the haptotaxis assays, the $Gsn^{-/-}$ osteoclasts were significantly hypomotile. The data in A represent three separate osteoclast preparations, and each experiment is the mean of 20–30 cell tracks. The data are mean ± SE. Asterisks indicate $P < 0.0001$. The data in B represent four separate osteoclast preparations, and four Transwells were counted for each experimental condition. Asterisk indicates $P < 0.01$.

other mild osteopetrotic states (Hayman et al., 1996). The osteoblastic parameters of bone modeling revealed no change in osteoblast number or perimeter (Table II). There was an increase in mineral appositional rate in $Gsn^{-/-}$ mice, but the bone formation rates were normal (Table II). Increased mineralization of the skeleton has been observed frequently in the osteopetroses, suggesting a link between osteoclast dysfunction and mineralization. The increase in the mineral appositional rate of $Gsn^{-/-}$ mice may have been due to increased activity of osteoblasts capable of forming bone matrix in an area covered by these cells. Therefore, conclusions regarding the cause of the increase in bone mass require studies of osteoblast function beyond the scope of this report, since development of a mouse endochondral osteoblast model is required.

Assessment of the Mechanical Strength of Bones

The imbalance between bone resorption and formation and the increased mineralization reported here may have affected bone strength, and the ability of the skeleton to resist damage (fracture) may be altered. To test this possibility, we performed four-point bending tests of mouse bones to assess their mechanical strength, as described in Materials and Methods. As shown in Fig. 11 and Table III, the $Gsn^{-/-}$ bones required greater energy and greater maximal displacement to produce femoral failure compared with the $Gsn^{+/+}$ femurs. Changes in bone stiffness resulting from over mineralization and decreased remodeling seen in some osteopetroses were not observed in the bones from the $Gsn^{-/-}$ mice.

Discussion

This report is the first demonstration that podosome assembly is critically gelsolin-dependent. The role of gelsolin in actin filament assembly and stimulus–response coupling associated with cell motility is well known (Stossel et al., 1985; Janmey and Stossel, 1987; Janmey et al., 1987; Stossel, 1989; Yin, 1989; Weeds and Maciver, 1993). However, most cells function well without gelsolin, indicating that gelsolin's functions are effectively substituted for in most cells by other actin severing or capping proteins. In these cells, attachment to matrix utilizes focal adhesions, and motility is often accomplished by lamellipodia. On the other hand, we demonstrate here that cells such as the osteoclast, which rely on podosomes for attachment and motility, are rendered hypomotile by the absence of gelsolin, and furthermore, the actin ring structures of the osteoclast that derive from podosome fusion are not formed. As a result, gelsolin deficiency is associated with abnormal actin cytoskeletal architecture, reduced rates of osteoclast motility, which contribute to reduced bone resorption in vivo, and podosome-associated signal transduction is blocked.

Gelsolin is the prototype of a large family of proteins that sever actin filaments, nucleate actin filament assembly, and block the fast exchanging end of actin filaments (Stossel, 1989). Therefore, the opportunity for redundancy of function in actin dynamics is high (Yin, 1987, 1989; Vandekerckhove and Vancompernolle, 1992; Weeds and Maciver, 1993; Schafer and Cooper, 1995) and the redundancy of actin-regulating proteins is manifested

Table III. Determination of Mechanical Strength of Femurs from $Gsn^{+/+}$ and $Gsn^{-/-}$ Mice

Parameter	$Gsn^{+/+}$	$Gsn^{-/-}$
Rigidity (Nmm/[mm/mm²])	1,284 ± 235	1,193 ± 249
Ultimate moment (Nmm)	39.3 ± 4.8	42.1 ± 4.8
Ultimate normalized displacement (mm/mm²)	0.054 ± 0.006	0.06 ± 0.006*
Energy (Nmm × [mm/mm²])	0.966 ± 0.204	1.284 ± 0.318‡

Data shown are mean ± SD of two experiments. There are eight animals per group.
*$P < 0.05$.
‡$P = 0.02$.

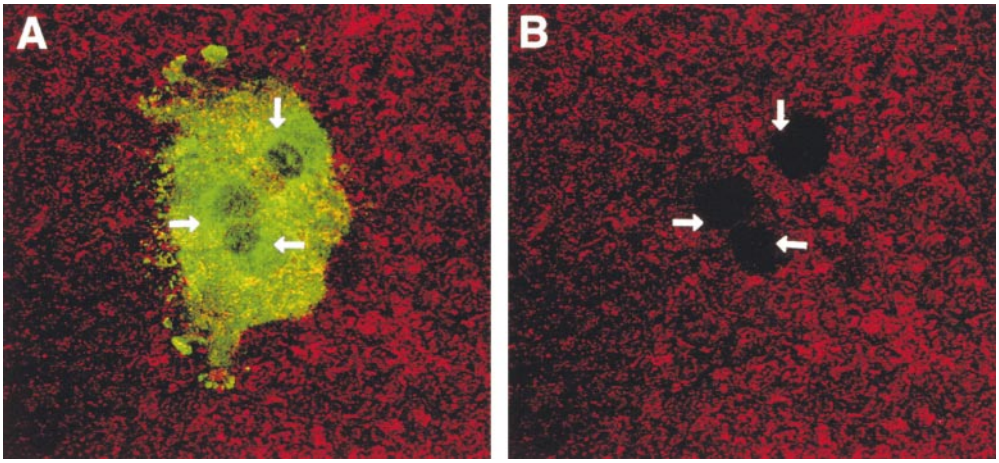

Figure 8. Polarization of the osteoclast plasma membrane as detected by distribution of the vacuolar H+ ATPase. (A) Confocal microscopy of an osteoclast derived from $Gsn^{-/-}$ cells. The section was taken at the level of the dentine slice as shown by the reflected light (red). The arrows point to areas of concentration of the H+ ATPase detected by the E11 antibody. (B) The areas of H+ ATPase concentration overlie a multiocular resorption pit produced by the osteoclast.

by the $Gsn^{-/-}$ mouse. Since gelsolin is not expressed during development, cell motility in support of development should be normal, and transgenic mice lacking gelsolin expression exhibit normal motility of embryonic fibroblasts (Witke et al., 1995). However, dermal fibroblasts from adult $Gsn^{-/-}$ mice have increased actin stress fiber size, decreased actin severing, and hypomotility. In addition, resting platelets isolated from $Gsn^{-/-}$ mice have an increased F-actin content, and they are slow to remodel their actin cytoskeleton when activated (Barkalow and Hartwig, 1995). According to the model of regulated treadmilling for regulation of actin dynamics through the filament-nucleating activity of the Arp 2/3 complex (Machesky and Insall, 1999), the findings in gelsolin deficiency are compatible with capping protein serving to complement for gelsolin deficiency with the only outcome being reduction in the rates of motility (Andre et al., 1989; Witke et al., 1995). Thus, our findings that gelsolin is required for podosome assembly is surprising. They establish that the podosome is a unique cell attachment structure, and that in its case, gelsolin capping of actin filaments cannot be substituted. The data also raise the question as to whether podosome assembly utilizes regulated treadmilling and the Arp 2/3 complex for actin filament elongation or whether gelsolin uncapping barbed ends is sufficient for this purpose.

$Gsn^{-/-}$ osteoclasts were adherent through novel cell–matrix interaction sites, e.g., vinculin-containing focal contacts distinct from focal adhesions, and they were able to polarize their actin cytoskeleton and plasma membranes sufficiently to enable bone resorption. These redundant mechanisms of actin regulation were sufficient for basal rates of bone resorption measured on dentine slices in vitro. However, $Gsn^{-/-}$ osteoclasts had a major decrease in motility in vitro, demonstrating that the redundant cell–matrix attachment mechanisms were unable to support the rates of assembly and disassembly observed in podosomes that enable high motility rates. This may be the critical component of the osteoclast phenotype in vivo, since the histomorphometric findings demonstrated that bone resorption measured by eroded perimeters was diminished. The findings of hypomotility in vitro and reduced bone resorption in vivo are compatible with the physiologic character of bone resorbing osteoclasts that display high motility rates. Therefore, our data suggest that motility is an important component of bone resorption.

Whereas hypomotility of leukocytes and fibroblasts was a central focus of the reported phenotype of $Gsn^{-/-}$ mice (Witke et al., 1995), these cells are motile through the process of cellular extensions, filopodia and lamellipodia, establishing new contacts, and pulling the trailing edge of the cell (Lauffenburger and Horwitz, 1996). Gelsolin has been shown to be an obligate downstream effector of rac-stimulated fibroblast motility (Azuma et al., 1998), where its severing of cortical actin is required for membrane ruffling, and the loss of gelsolin severing may have produced the decrease in motility. In the studies reported here related to the absence of podosome assembly, the basis for the defect appears related to gelsolin-capping function that must be required in order for the podosome structure to be completed. Several studies have shown a relationship between gelsolin content and cell migration (Chaponnier et al., 1990; Cunningham et al., 1991; Arora and McCulloch, 1996; Kwiatkowski, 1999). Increasing gelsolin content in cultured fibroblasts by transfection proportionally enhances the rate of cell migration toward a chemoattractant (Cunningham et al., 1991; Arora and McCulloch, 1996). Large increases in gelsolin content are also associated with the enhanced motility exhibited during differentiation of myeloid cell lines into macrophage-like cells (Kwiatkowski, 1988). However, it has been shown that high gelsolin content is associated with reduced cell migration and increased adhesion in smooth muscle and mammary carcinoma cells (Chaponnier and Gabbiani, 1989; Chaponnier et al., 1990). Thus, the capping or severing functions of gelsolin may be variably important depending upon the cell type, but only in the case of podosome assembly is gelsolin critical.

Osteoclasts are unique in that their mechanism of cell motility is podosome based. They do not express focal adhesions, and they use the speed of podosome assembly and disassembly to generate high rates of motility. Gelsolin is present in podosomes of osteoclasts but not in focal adhesions (Marchisio et al., 1987). The greater reliance on podosomes for cell attachment in osteoclasts called immediate attention to podosome absence in $Gsn^{-/-}$ osteoclasts.

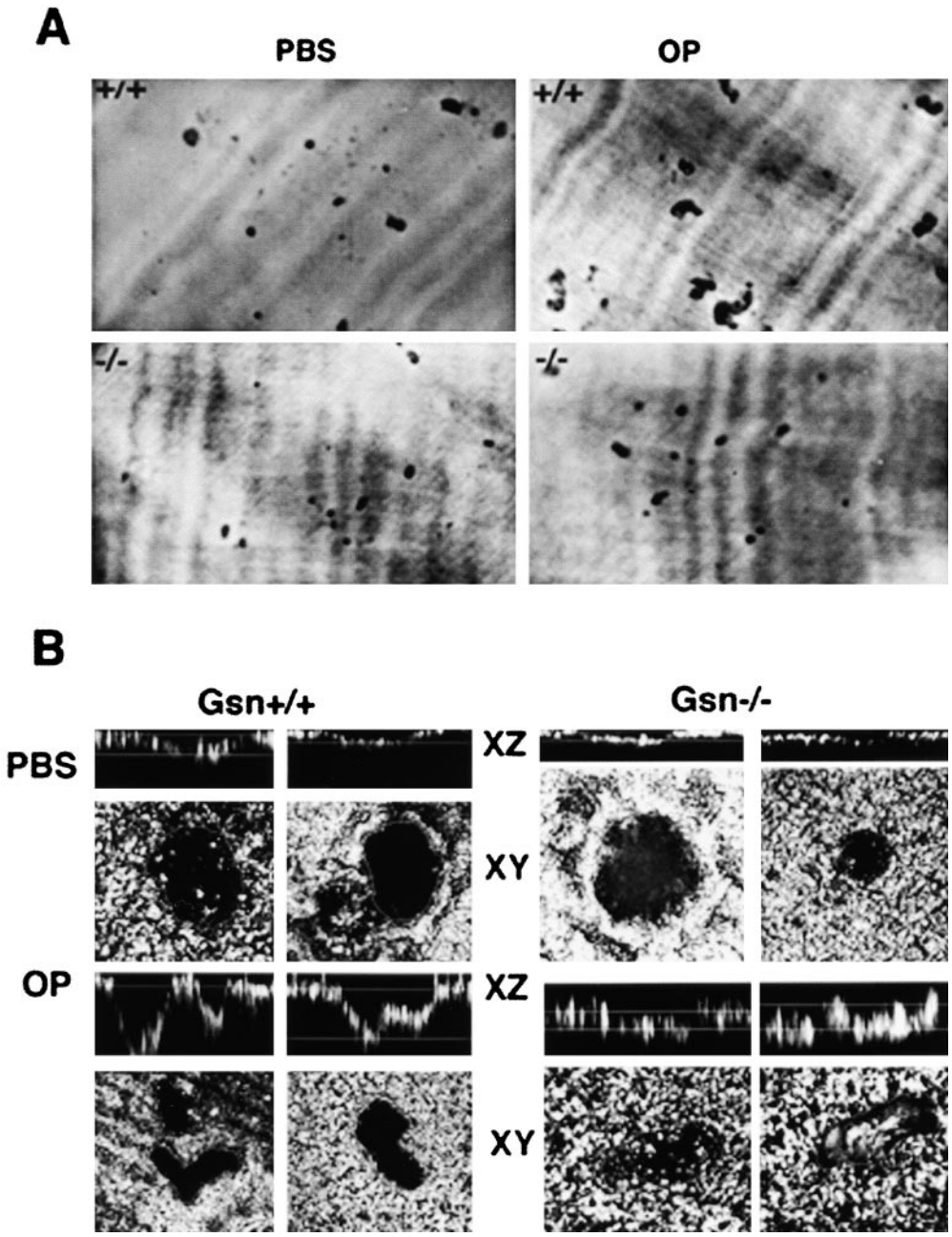

Figure 9. Bone resorbing activity of osteoclasts isolated from $Gsn^{+/+}$ and $Gsn^{-/-}$ mice. Osteoclasts were plated on dentine slices as described in Materials and Methods, and the formation of resorption pits was assessed after 48 h. In low-power views of dentine slices stained by acid hematoxylin, resorption pits were seen as dark spots as shown in A. In the dentine slices on which $Gsn^{+/+}$ osteoclasts (+/+) were added, there were numerous resorption pits that increased in size and complexity by treatment with OP. In osteoclasts derived from cells of $Gsn^{-/-}$ mice (−/−), resorption pits were small and not affected by OP treatment. (B) Confocal images of the pit. Individual resorption pits were assessed by confocal microscopy for pit depth (XZ) and pit area (XY). In dentine slices on which $Gsn^{-/-}$ osteoclasts were plated, pit depth was diminished. Pit depth was remarkably increased by treatment with OP in $Gsn^{+/+}$ osteoclasts, but it was unaffected by OP in the slices with $Gsn^{-/-}$ osteoclasts. Group data of pit depth (XZ scans) and pit area (XY scans) from confocal microscopy of pits on multiple dentine slices from three osteoclast preparation are shown in Table I.

Even the actin ring structure of the bone resorbing osteoclast is a coalescence of dense rows of podosomes, and they were absent in $Gsn^{-/-}$ osteoclasts. Osteoclasts are uniquely motile in that they continue to resorb bone beneath one area of the cell undersurface while another area is reorganizing and moving (Taylor et al., 1989). The result is the production of complex resorption pits with a serpentine character (Taylor et al., 1989). The rapidity of podosome assembly and disassembly enables this feature of coordinating cell function with motility (Kanehisa and Heersche, 1988; Kanehisa et al., 1990), another property shared between metastatic cancer cells and osteoclasts. Thus, as reported herein, impaired motility of $Gsn^{-/-}$ osteoclasts is associated with diminished rates of bone resorption.

Gelsolin plays a key role in integrin-based signaling through podosomes as it is organized in a signaling complex containing PI3-K, $pp^{60c\text{-}src}$, and other signaling molecules (Chellaiah and Hruska, 1996; Chellaiah et al., 1998). As shown here, this complex is expressed in murine wild-type osteoclasts, and the role of this complex is demonstrated by the absence of response to OP in the $Gsn^{-/-}$ osteoclasts. The receptor for OP signaling is the $\alpha_v\beta_3$ integrin (Chellaiah and Hruska, 1996; Chellaiah et al., 1998), also localized to the osteoclast podosome (Zambonin-Zallone et al., 1989). In the $Gsn^{-/-}$ osteoclasts, $\alpha_v\beta_3$ was expressed in the unique focal contacts, and OP was secreted into the resorption space (Chellaiah, M., unpublished observations). Thus, the major deficiency in the response to OP was the organization of signaling around gelsolin in the podosome for motility. The $Gsn^{-/-}$ osteoclasts organized

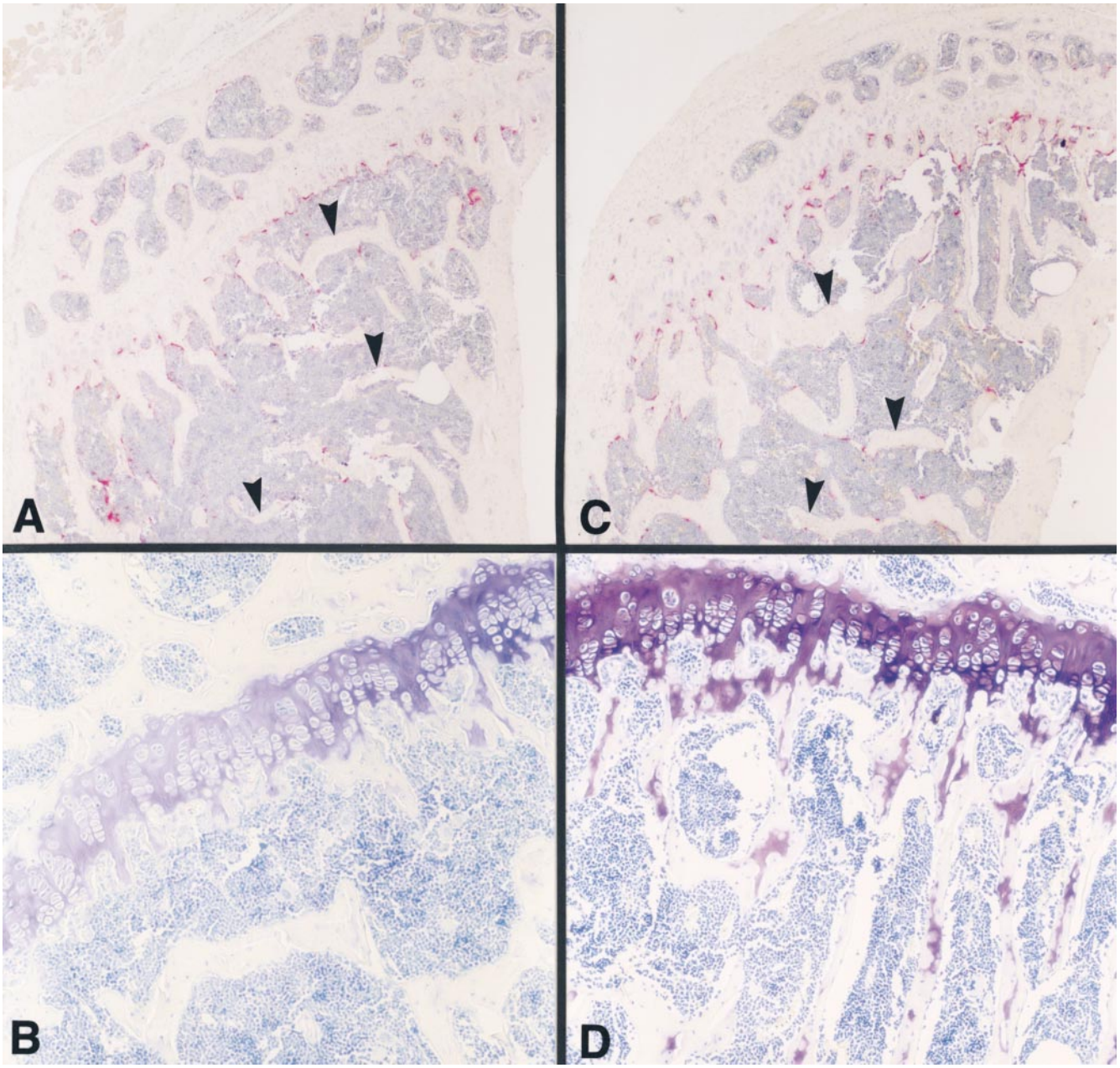

Figure 10. Histomorphometric analysis of proximal tibial sections of $Gsn^{-/-}$ and $Gsn^{+/+}$ mice. Proximal tibial sections of bone isolated from 14-wk-old $Gsn^{+/+}$ (A and B) and $Gsn^{-/-}$ (C and D) mice were stained for TRAP (A and C) or with toluidine blue (B and D). (A and C) TRAP staining. Numerous osteoclasts were visible in the primary spongiosa and on the surfaces of metaphyseal trabeculae in both +/+ (A) and −/− mice (C). The number of TRAP-positive osteoclasts below the growth plate in −/− mice tends to be increased, giving the appearance of a double row of cells as the trabeculae develop from the primary spongiosa (C). The trabecular bone volume in the metaphysis of the −/− mice was increased (shown by arrows; compare A and C; see Table II). (B and D) Toluidine blue staining. The metaphyseal trabeculae of −/− mice (D) had retained cartilage-derived proteoglycan.

their cytoskeleton and polarized sufficiently to resorb bone. Thus, signal transduction through $\alpha_v\beta_3$ and the focal contacts that substitute for podosomes may explain the basal rates of bone resorption in vitro, and osteoclast function sufficient to support development of the skeleton and normal rates of endochondral bone growth in vivo.

Histomorphometric analysis of bones from $Gsn^{-/-}$ mice documented reduced resorption of calcified cartilage in the epiphyses of the long bones. The epiphyses were mildly disorganized with increased cartilage matrix. The metaphyseal bone trabeculae were thicker than those observed in $Gsn^{+/+}$ bones, and they had retained cartilage proteoglycans. Cancellous bone area was increased, and the eroded surface area was decreased. Both trabecular and cortical bone were thicker, and the cause of this appeared to be decreased osteoclast function in the presence of normal osteoblast function. Osteoblast number and surfaces were normal, as were bone formation rates, which

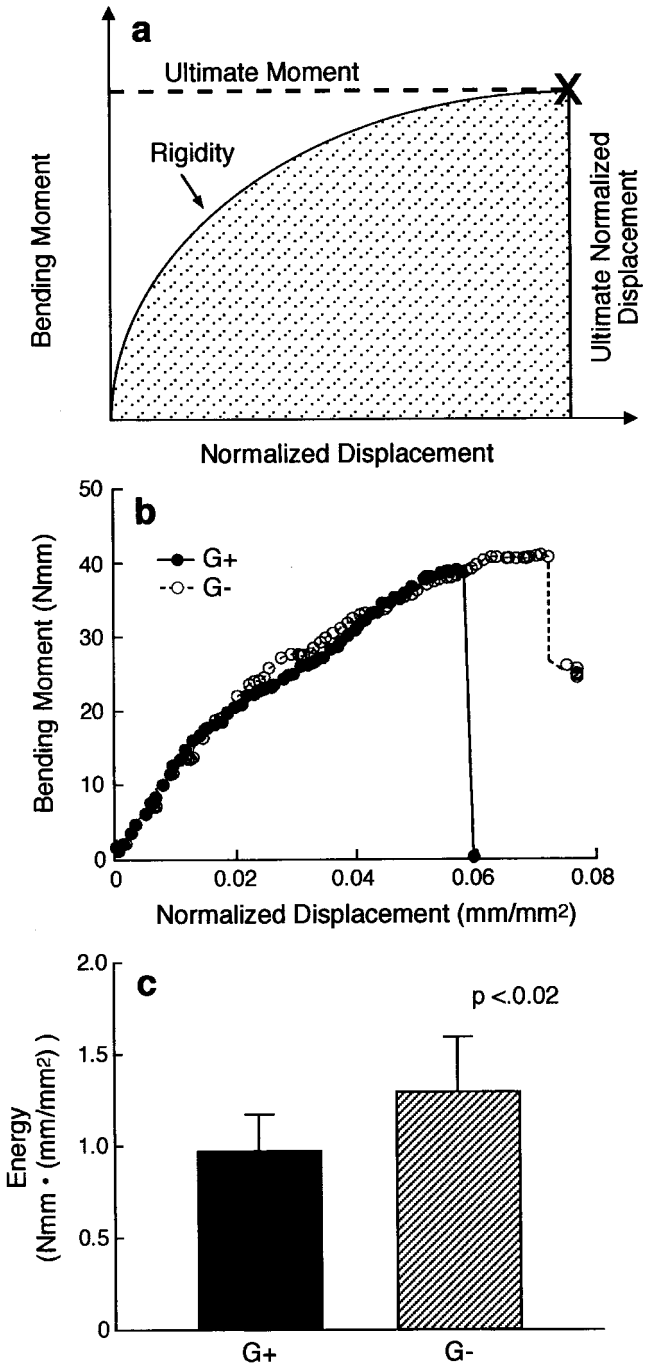

Figure 11. Mechanical strength of femurs from $Gsn^{+/+}$ and $Gsn^{-/-}$ mice. (a) Graphic representation of the data generated by four-point bending test. The slope of the line relating bending and displacement is a reflection of stiffness or rigidity, and the area under the curve is the energy required to produce failure. (b) The ultimate moment-displacement curves for +/+ and −/− femurs. The normalized displacement at failure (ultimate) was greater in the $Gsn^{-/-}$ femurs (see Table II). (c) The energy required to produce failure was greater in the femurs from $Gsn^{-/-}$ mice (see Table III).

tended to be elevated although not significantly. The deficiency in osteoclast function was not sufficient to affect endochondral bone growth, and the shortening and clubbing of the femurs reported in some osteopetrotic states was not observed (Marks, 1989; Hayman et al., 1996). The effect of thicker trabeculae and cortices on bone strength was an increase in load required to produce failure, and an increase in the ultimate normalized displacement to produce fracture.

Skeletal diseases characterized by sclerosis resulting from reduced osteoclast-mediated bone resorption are referred to as the osteopetroses (Marks, 1989). Osteopetrosis is a heterogeneous group of disorders that range in severity from lethal to the very mild disorder reported here. The lethal disorders result from an absence of marrow cavity formation and the limited development of hematopoiesis. The milder disorders are associated with shortening and deformity of the long bones and axial skeleton, but tooth eruption, hearing, and skull plate development (Hayman et al., 1996). The osteopetrosis reported here is even milder in that endochondral bone lengths were normal. The milder forms of osteopetrosis have been associated with significant effects on skeletal mineralization demonstrating progressive increases in bone density as observed here by the increase in mineral apposition rate (Hayman et al., 1996).

An effect of osteoclast dysfunction on mineralization was suggested in the Acp5 TRAP-deficient homozygous mutant mice. TRAP may dephosphorylate OP in the osteoclast resorption space (Ek-Rylander et al., 1994), and as a result increase mineralization by affecting the role of OP in the bone formation that follows cessation of osteoclast function.

Thus, the findings reported here of thickened calcified cartilage trabeculae, delayed cartilage resorption, and diminished eroded perimeters demonstrate a mild osteopetrosis that was not developmentally important nor sufficient to affect growth, but it was sufficient to increase trabecular and cortical bone thickness with age resulting in increased skeletal strength. The findings reported here resemble the long-term outcome of aminobisphosphonate administration to humans, producing a mild imbalance between bone resorption and bone formation that results in an increase in bone mass (Liberman, 1995; Saag et al., 1998). As a result, these studies suggest that the gelsolin-based signaling complex of the osteoclast podosome is an attractive target for pharmacologic regulation of bone resorption.

The authors wish to thank Dr. Stephen Gluck for the E11 antibody to the 32-kD subunit of the vacuolar H+ ATP osteoclast proton pump; Drs. John Freeman and Brian Bennett for assistance with the confocal microscopy; Mrs. Crystal Idleburg for assistance with the bone sectioning and staining; and Kathy Jones and Helen Odle for secretarial assistance.

This work was supported by grant AR41677 (K.A. Hruska and M. Chellaiah) from the National Institutes of Health and the Monsanto/Washington University consortium.

Submitted: 21 September 1999
Revised: 21 December 1999
Accepted: 18 January 2000

References

Andre, E., M. Brink, G. Gerisch, G. Isenberg, A. Noegel, M. Schleicher, J.E. Segali, and E. Wallraff. 1989. A *Dictyostelium* mutant deficient in severin, an F-actin fragmenting protein, shows normal motility and chemotaxis. *J. Cell Biol.* 108:985–995.

Arora, P.D., and C.A.G. McCulloch. 1996. Dependence of fibroblast migration on actin severing activity of gelsolin. *J. Biol. Chem.* 271:20516–20523.

Azuma, T., W. Witke, T.P. Stossel, J.H. Hartwig, and D.J. Kwiatkowski. 1998. Gelsolin is a downstream effector of rac for fibroblast motility. *EMBO (Eur. Mol. Biol. Organ.) J.* 17:1362–1370.

Barkalow, K., and J.H. Hartwig. 1995. Actin cytoskeleton. Setting the pace of cell movement. *Curr. Biol.* 5:1000–1002.

Blair, H.C., S.L. Teitelbaum, R. Ghiselli, and S. Gluck. 1989. Osteoclastic bone resorption by a polarized vacuolar proton pump. *Nature.* 245:855–857.

Boyce, B.F., T. Yoneda, C. Lowe, P. Soriano, and G.R. Mundy. 1992. Requirement of pp60c-src expression for osteoclasts to form ruffled borders and resorb bone in mice. *J. Clin. Invest.* 90:1622–1627.

Buck, C.A., and A.F. Horwitz. 1987. Integrin, a transmembrane glycoprotein complex mediating cell-substratum adhesion. *J. Cell Sci. Suppl.* 8:231–250.

Chaponnier, C., and G. Gabbiani. 1989. Gelsolin modulation in epithelial and stromal cells of mammary carcinoma. *Am. J. Pathol.* 134:597–603.

Chaponnier, C., O. Kocher, and G. Gabbiani. 1990. Modulation of gelsolin content in rat aortic smooth muscle cells during development, experimental intimal thickening and culture. An immunohistochemical and biochemical study. *Eur. J. Biochem.* 190:559–565.

Chellaiah, M., and K.A. Hruska. 1996. Osteopontin stimulates gelsolin associated phosphoinositide levels and PtdIns 3-hydroxyl kinase. *Mol. Biol. Cell.* 7:743–753.

Chellaiah, M., C. Fitzgerald, E.J. Filardo, D.A. Cheresh, and K.A. Hruska. 1996. Osteopontin activation of c-*src* in human melanoma cells requires the cytoplasmic domain of the integrin α_v subunit. *Endocrinology.* 137:2432–2440.

Chellaiah, M., C. Fitzgerald, U. Alvarez, and K. Hruska. 1998. C-*src* is required for stimulation of gelsolin associated PI3-K. *J. Biol. Chem.* 273:11908–11916.

Cunningham, C.C., T.P. Stossel, and D.J. Kwiatkowiski. 1991. Enhanced motility in NIH3T3 fibroblasts that overexpress gelsolin. *Science.* 251:1233–1236.

Ek-Rylander, B., M. Flores, M. Wendel, D. Heinegard, and G. Andersson. 1994. Dephosphorylation of osteopontin and bone sialoprotein by osteoclastic tartrate-resistant acid phosphatase. *J. Biol. Chem.* 269:14853–14856.

Gupta, A., J.C. Edwards, and K.A. Hruska. 1996. Cellular distribution and regulation of NHE-1 isoform of the Na-H exchanger in the avian osteoclast. *Bone.* 18:87–95.

Hayman, A.R., S.J. Jones, A. Boyde, D. Foster, W.H. Colledge, M.B. Carlton, M.J. Evans, and T.M. Cox. 1996. Mice lacking tartrate-resistant acid phosphatase (Acp 5) have disrupted endochondral ossification and mild osteopetrosis. *Development.* 122:3151–3162.

Hemken, P., X.-L. Guo, A.-Q. Wang, K. Zhang, and S. Gluck. 1992. Immunologic evidence that vacuolar H+ ATPases with heterogeneous forms of Mr = 31,000 subunit have different membrane distributions in mammalian kidney. *J. Biol. Chem.* 267:9948–9957.

Horton, M.A., P. Townsend, and S. Nesbitt. 1996. Cell surface attachment molecules in bone. *In* Principles of Bone Biology. J.P. Bilezikian, L.G. Raisz, and G.A. Rodan, editors. Academic Press, San Diego, CA. 217–230.

Janmey, P.A., and T.P. Stossel. 1987. Modulation of gelsolin function by polyphosphoinositol(4,5)-bisphosphate. *Nature.* 325:362–364.

Janmey, P.A., K. Iida, H.L. Yin, and T.P. Stossel. 1987. Polyphosphoinositide micelles and polyphosphoinositide-containing vesicles dissociate endogenous gelsolin-actin complex and promote actin assembly from the fast growing end of actin filaments blocked by gelsolin. *J. Biol. Chem.* 262:12228–12236.

Jepsen, K.J., S.A. Goldstein, J.L. Kuhn, M.B. Schaffler, and J. Bonadio. 1996. Type-1 collagen mutation compromises the post-yield behavior of Mov13 long bone. *J. Orthop. Res.* 14:493–499.

Jilka, R.L., R.S. Weinstein, K. Takahashi, A.M. Parfitt, and S.C. Manolagas. 1996. Linkage of decreased bone mass with impaired osteoblastogenesis in a murine model of accelerated senescence. *J. Clin. Invest.* 97:1732–1740.

Kanehisa, J., and J.N.M. Heersche. 1988. Osteoclastic bone resorption: in vitro analysis of the rate of resorption and migration of individual osteoclasts. *Bone.* 9:73–79.

Kanehisa, J., T. Yamanaka, S. Doi, K. Turksen, J.N.M. Heersche, J.E. Aubin, and H. Takeuchi. 1990. A band of F-actin containing podosomes is involved in bone resorption by osteoclasts. *Bone.* 11:287–293.

Kwiatkowski, D.J. 1988. Predominant induction of gelsolin and actin-binding protein during myeloid differentiation. *J. Biol. Chem.* 263:13857–13862.

Kwiatkowski, D.J. 1999. Functions of gelsolin: motility, signaling, apoptosis, cancer. *Curr. Opin. Cell Biol.* 11:103–108.

Lakkakorpi, P.T., and H.K. Vaananen. 1991. Kinetics of the osteoclast cytoskeleton during the resorption cycle in vitro. *J. Bone Miner. Res.* 6:817–826.

Lakkakorpi, P.T., M.H. Helfrich, M.A. Horton, and H.K. Vaananen. 1993. Spatial organization of microfilaments and vitronectin receptor, $\alpha_v\beta_3$, in osteoclasts. *J. Cell Sci.* 104:663–670.

Lakkakorpi, P.T., G. Wesolowski, L. Limolo, G.A. Rodan, and S.B. Rodan. 1997. Phosphatidylinositol 3-kinase association with the osteoclast cytoskeleton and its involvement in osteoclast attachment and spreading. *Exp. Cell Res.* 237:296–306.

Lauffenburger, D.A., and A.F. Horwitz. 1996. Cell migration: a physically integrated molecular process. *Cell.* 84:359–369.

Liberman, U.A. 1995. Effect of oral alendronate on bone mineral density and the incidence of fractures in postmenopausal osteoporosis. *N. Engl. J. Med.* 333:1437–1443.

Lu, M., W. Witke, D.J. Kwiatkowski, and K.S. Kosik. 1997. Delayed retraction of filopodia in gelsolin null mice. *J. Cell Biol.* 138:1279–1287.

Machesky, L.M., and R.H. Insall. 1999. Signaling to actin dynamics. *J. Cell Biol.* 146:267–272.

Maejima-Ikeda, A., M. Aoki, K. Tsuritani, K. Kamioka, K. Hiura, T. Miyoshi, H. Hara, T. Takano-Yamamoto, and M. Kumegawa. 1997. Chick osteocyte-derived protein inhibits osteoclastic bone resorption. *Biochem. J.* 322:245–250.

Marchisio, P.C., L. Naldini, D. Cirillo, M.V. Primavera, A. Teti, and A. Zambonin-Zallone. 1984. Cell-substratum interactions of cultured avian osteoclasts is mediated by specific adhesion structures. *J. Cell Biol.* 99:1696–1705.

Marchisio, P.C., D. Cirillo, A. Teti, A. Zambonin Zallone, and G. Tarone. 1987. Rous sarcoma virus-transformed fibroblasts and cells of monocytic origin display a peculiar dot-like organization of cytoskeletal proteins involved in microfilament-membrane interaction. *Exp. Cell Res.* 169:202–214.

Marks, S.C., Jr. 1989. Osteoclast biology: lessons from mammalian mutations. *Am. J. Med. Genet.* 34:43–54.

Nakamura, I., T. Sasaki, S. Tanaka, N. Takahashi, E. Jimi, T. Kurokawa, Y. Kita, S. Ihara, T. Suda, and Y. Fukui. 1997. Phosphatidylinositol-3 kinase is involved in ruffled border formation in osteoclasts. *J. Cell Physiol.* 172:230–239.

Parfitt, A.M., M.K. Drezner, F.H. Glorieux, J.A. Kanis, H. Malluche, P.J. Meunier, S.M. Ott, and R.R. Recker. 1987. Bone histomorphometry: standardization of nomenclature, symbols, and units. *J. Bone Miner. Res.* 2:595–610.

Rodriguez Fernandez, J.L., B. Geiger, D. Salomon, and A. Ben-Ze'ev. 1992. Overexpression of vinculin suppresses cell motility in BALB/c 3T3 cells. *Cell Motil. Cytoskelet.* 22:127–134.

Rodriguez Fernandez, J.L., B. Geiger, D. Salomon, and A. Ben-Ze'ev. 1993. Suppression of vinculin expression by antisense transfection confers changes in cell morphology, motility, and anchorage-dependent growth of 3T3 cells. *J. Cell Biol.* 122:1285–1294.

Saag, K.G., R. Emkey, T.J. Schnitzer, J.P. Brown, F. Hawkins, S. Goemaere, G. Thamsborg, U.A. Liberman, P.D. Delmas, M.-P. Malice, et al. 1998. Alendronate for the prevention and treatment of glucocorticoid-induced osteoporosis. *N. Engl. J. Med.* 339:292–299.

Schafer, D.A., and J.A. Cooper. 1995. Control of actin assembly at filament ends. *Annu. Rev. Cell Dev. Biol.* 11:497–518.

Schwartzberg, P.L., L. Xing, O. Hoffmann, C.A. Lowell, L. Garrett, B.F. Boyce, and H.E. Varmus. 1997. Rescue of osteoclast function by transgenic expression of kinase-deficient Src in *Src*−/− mutant mice. *Genes Dev.* 11: 2835–2844.

Senger, D.R., S.R. Ledbetter, K.P. Claffey, A. Papadopoulos-Sergiou, C.A. Perruzzi, and M. Detmar. 1996. Stimulation of endothelial cell migration by vascular permeability factor/vascular endothelial growth factor through cooperative mechanisms involving the $\alpha_v\beta_3$ integrin, osteopontin, and thrombin. *Am. J. Pathol.* 149:293–305.

Shioi, A., F.P. Ross, and S.L. Teitelbaum. 1994. Enrichment of generated murine osteoclasts. *Calcif. Tissue Int.* 55:387–394.

Steimle, P.A., J.D. Hoffert, N.B. Adey, and S.W. Craig. 1999. Polyphosphoinositides inhibit the interaction of vinculin with actin filaments. *J. Biol. Chem.* 274:18414–18420.

Stossel, T.P. 1989. From signal to pseudopod. How cells control cytoplasmic actin assembly. *J. Biol. Chem.* 264:18261–18264.

Stossel, T.P., C. Chaponnier, R.M. Ezzell, J.H. Hartwig, P.A. Janmey, D.J. Kwiatkowski, S.E. Lind, D.B. Smith, F.S. Southwick, H.L. Yin, and K.S. Zaner. 1985. Nonmuscle actin-binding proteins. *Annu. Rev. Cell Biol.* 1:353–402.

Takahashi, S., S. Goldring, M. Katz, S. Hilsenbneck, R. Williams, and G.D. Roodman. 1995. Down regulation of calcitonin receptor mRNA expression by calcitonin during human osteoclast-like cell differentiation. *J. Clin. Invest.* 95:167–171.

Taylor, M.L., A. Boyde, and S.J. Jones. 1989. The effect of fluoride on the patterns of adherence of osteoclasts cultured on and resorbing dentine: a 3-D assessment of vinculin-labelled cells using confocal optical microscopy. *Anat. Embryol.* 180:427–435.

Teti, A., P.C. Marchisio, and A. Zambonin-Zallone. 1991. Clear zone in osteoclast function: role of podosomes in regulation of bone-resorbing activity. *Am. J. Physiol.* 261:C1–C7.

Turksen, K., J. Kanehisa, M. Opas, J.N. Heersche, and J.E. Aubin. 1988. Adhesion patterns and cytoskeleton of rabbit osteoclasts on bone slices and glass. *J. Bone Miner. Res.* 3:389–400.

Vandekerckhove, J., and K. Vancompernolle. 1992. Gelsolin modulation in epithelial and stromal cells of mammary carcinoma. *Curr. Opin. Cell Biol.* 4:36–42.

Weeds, A., and S. Maciver. 1993. F-actin capping proteins. *Curr. Opin. Cell Biol.* 5:63–69.

Weinstein, R.S., R.L. Jilka, A.M. Parfitt, and S.C. Manolagas. 1997. The effects of androgen deficiency on murine bone remodeling and bone mineral density are mediated via cells of the osteoblastic lineage. *Endocrinology.* 138: 4013–4021.

Wesolowski, G., L.T. Duong, T. Lakkakorpi, R.M. Nagy, K.I. Tezuka, H. Tanaka, G.A. Rodan, and S.B. Rodan. 1995. Isolation and characterization of highly enriched perfusion mouse osteoclastic cells. *Exp. Cell Res.* 219: 679–686.

Witke, W., A. Sharpe, J. Hartwig, T. Azuma, T. Stossel, and D. Kwiatkowski. 1995. Hemostatic, inflammatory, and fibroblast responses are blunted in mice lacking gelsolin. *Cell.* 81:41–51.

Wu, H., S.B. Kanner, A.B. Reynolds, R.R. Vines, and J.T. Parson. 1991. Identification and characterization of a novel cytoskeleton associated $pp^{60c\text{-}src}$ substrate. *Mol. Cell. Biol.* 11:5113–5124.

Xu, W., J.-L. Coll, and E.D. Adamson. 1998. Rescue of the mutant phenotype by reexpression of full-length vinculin in null F9 cells; effects on cell locomotion by domain deleted vinculin. *J. Cell Sci.* 111:1535–1544.

Yin, H.L. 1987. Gelsolin: calcium and phosphoinositide regulated actin modulating protein. *Bioessays.* 7:176–179.

Yin, H.L. 1989. Calcium and polyphosphoinositide regulation of actin network structure by gelsolin. *Adv. Exp. Med. Biol.* 255:315–323.

Zambonin-Zallone, A., A. Teti, M.V. Primavera, L. Naldini, and P.C. Marchisio. 1983. Osteoclasts and monocytes have similar cytoskeletal structures and adhesion property in vitro. *J. Anat.* 137:57–70.

Zambonin-Zallone, A., A. Teti, M. Grano, A. Rubinacci, M. Abbadini, M. Gaboli, and C. Marchisio. 1989. Immunocytochemical distribution of extracellular matrix receptors in human osteoclasts: a beta3 integrin is co-localized with vinculin and talin in the podosomes of osteoclastoma giant cells. *Exp. Cell Res.* 182:645–652.

Zhang, D., N. Udagawa, I. Nakamura, H. Murakami, S. Saito, K. Yamasaki, Y. Shibasaki, N. Morij, S. Narumiya, N. Takahashi, and T. Suda. 1995. The small GTP-binding protein, rho p21, is involved in bone resorption by regulating cytoskeletal organization in osteoclasts. *J. Cell Sci.* 108:2285–2292.